further generalized. Thus, the efficiency of the shape choice can be measured under the form of generalized cost, while the allowable stress state can be appreciated according to a procedure similar to that of failure theory, by a function connecting the stress tensor components.

REFERENCES

1. Priscu, R. 1974. *Hydraulic Structures*. Bucharest (in Romanian).
2. Micula, G. 1978. *Spline Function and Applications*. Bucharest (in Romanian).
3. Wilson, E.L., K.J. Bathe & P.E. Peterson 1973. *SAP IV – A Structural Analysis Program for Static and Dynamic Response of Linear Systems*. Berkeley, USA.
4. Clough, R.W., J.M. Raphael & S. Mojtahedi 1973. *ADAP – A Computer Program for Static and Dynamic Analysis of Arch Dams*. Berkeley, USA.
5. Suprovici, P. 1986. Concrete dam optimization. PhD thesis, Civil Engineering Institute, Bucharest (in Romanian).
6. Suprovici, P. 1986. *OPTAR – A Computer Program for Arch Dams Optimization. Users Guide*. ITCI, Bucharest.

3.2 SEARCH FOR ARCH DAMS WITH OPTIMAL SHAPE

L.M.C. Simões, J.A.M. Lapa & J.H. Negrão

INTRODUCTION

There is an important class of structural optimization problems in which the shape of the structure is to be determined. The exterior and interior boundary shapes of the structure should be controlled in such an optimization algorithm. One of the applications of those concepts is the design of a doubly curved arch dam.

Since within the design process the shapes vary continuously, careful consideration has to be paid to describing the changing boundary shape, in order to maintain an adequate finite element mesh, enhance the accuracy of the sensitivity analysis, impose proper constraints and use available optimization methods to solve the shape design problem.

Arch dams were first given cylindrical shapes.[1] These were followed by constant angle shapes where the arches become parabolic or elliptic. The arches were plotted three centered, showing a decrease of curvature towards the abutments. This type of layout is based on the discussion of arch load results, especially those of trial load calculations.[2,3] Early research investigations into the problem of design have dealt mainly with membrane type solutions.[4,5] These methods ignore foundation elasticity and bending stresses and consider a single loading condition. However, membrane type solutions may provide useful starting points for more comprehensive studies, providing these include constraints on geometry such as minimum thicknesses, maximum overhangs, effects of bending and foundation elasticity.

Some optimization work was carried out by employing membrane shell theory,[6] but the results are only meaningful when applied to special dam shapes and boundary

conditions. Difficulties in eliminating tensile stresses (even under a single loading case) were also experienced using thin shell theory[7] to optimize a doubly curved arch dam. One method of overcoming this difficulty is to create a hinged boundary condition.

In order to obtain accurate double curvature shell finite elements, the usual course is to base the solution upon a relatively high order plate bending element coupled with a membrane element of comparable accuracy,[8] e.g. a quartic bending element (doubly curved thin shell) with a linear strain membrane (membrane element). This element can readily be applied to arbitrary shell shapes by integrating over the area given by the plane containing the corner nodes. It uses a facet element transformation to map the global displacement at each node to local values and the quadratic interpolation to define the surface slope variation through the element.[9] Although sufficiently accurate, these results show a slow rate of convergence, as expected.

In the free form method[10] (finite element based), a finite number of points located on the surface is used to define the structure, and alternative shapes are obtained by simply adjusting one or more coordinate points. Curve fitting techniques were required to describe curves passing through the free-form points. As an optimality criterion, it was found that subsequent shapes, based on the center line of thrust of the previous shape, converged rapidly to a much improved solution. Parametric studies[11] have been conducted using a much simpler formulation, using the radial adjustment method for stress determination (arch-cantilever).

Results from three-dimensional shape optimization of arch dams reported so far, use as a method of obtaining a solution, a sequential linear programming algorithm associated with either a 8 node[12] or a 20 node[13] isoparametric element. An automatic mesh generation and refinement has not yet been used and the shape function consists of either cross-sectional shape control[13] or polynomials.[12]

It is the purpose of this paper to describe neglected aspects of the design in order to point out areas where future enhancements should be made.

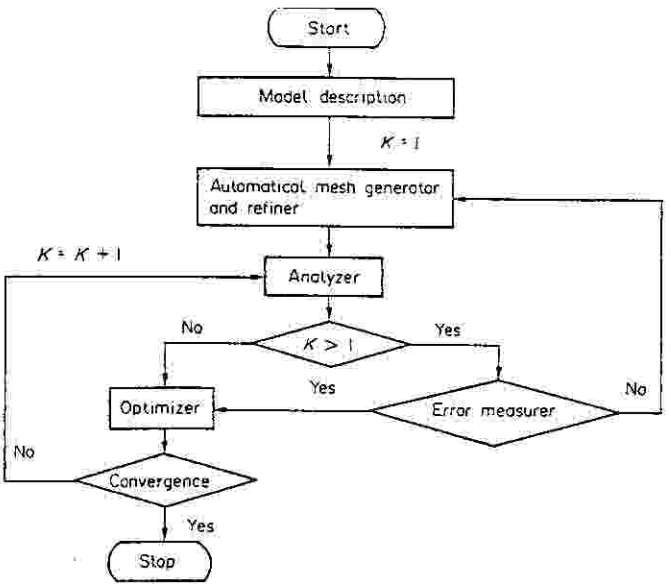

Figure 1.

MATHEMATICAL PROGRAMMING REPRESENTATION

1 *Statement of the problem*

The problem is to determine some or all of the following aspects of an arch dam:

(a) the shape and location (within a given area);

(b) the height;

(c) the construction materials properties (e.g. elastic modulus, concrete strength);

in order to maximize a merit function expressing the cost (volume) and functional usefulness of the structure in the terms given, subject to practical constraints on the behaviour and geometry.

The shape optimization can be stated in the standard form as:

$$\min v(s) \tag{1}$$

$$st\ g_i(s) \leq 0\ ;\ i = 1,\text{NBC} \tag{2}$$

$$s_k^L \leq s_k \leq s_k^U\ ;\ k = 1,\text{NSV} \tag{3}$$

$$d_j^L \leq \sum_{k=1,\text{NSV}} d_{kj}\, s_k \leq d_j^U\ ;\ j = 1,\text{NGC} \tag{4}$$

where $v(s)$ is the objective function, g_i the constraint function describing the i^{th} structural response; s is a vector defining the shape of the structure and s_k^L, s_k^U are the lower or upper limits on the shape which may reflect fabrication requirements or analysis limitations. The shape variable s may also be linked by linear explicit constraints which are introduced to deal with various geometrical requirements such as boundary slope continuity. NBC is the number of behavioural constraints, NSV the number of shape variables and NGC the number of geometrical constraints.

To summarize the design process of the shape optimization of an arch dam, a simple flow chart is given in Figure 1.

2 *Objective function*

The overall objective of an arch dam design is to achieve an economic and safe solution. It is difficult to quantify many of the factors on which the objective function depends. The factor which is most readily and conveniently evaluated is the cost (directly associated with the concrete volume). A cost-benefit analysis for an arch dam would include consideration of some or all of the following:

(a) The value of the reservoir capacity. This is a function of the irrigation, domestic, recreational and power generation demands and should also include the value of the dam as an essential element in flood control. This function can be expressed as a function of the dam height;

(b) The cost of the reservoir (excluding the dam structure). This function may also be formulated in terms of the dam height.

(c) The cost of the dam structure. This function includes the construction and material costs, sometimes not easily defined, although they can be considered proportional to the volume of concrete. In this study, it is not intended to include all the factors affecting the economics of a design, e.g. construction material, discharge safety equipment (spillways, outlet works, etc.). The objective in shaping the dam then reduces to the minimization of the concrete volume. This objective is assumed to lead to the following benefits: minimization of the concrete material cost, minimization of the excavation cost and

reduction of the construction period. The volume of the dam is thus given by the sum of the volumes of the finite elements and will be adopted in the sequel.

Alternatively, the stress field can be optimized: maximum compressive stresses in most of the volume and minimum or nil tensile stresses. For reasons of foundation security, the maximum overhangs of the dam and the angle of inclination of the arch thrust could also be minimized. If this is done, care must be taken that the shell design is not too shallow.

3 *Constraint functions*

Constraint functions must lead to a safe and functional design.

Thickness constraints are imposed in the form,

$$-p_j + p_{\min} \leq 0 \; ; \; p_j - p_{\max} \leq 0 \tag{5}$$

where p_j, $p_{\min}$ and $p_{\max}$ are the thickness of the dam at any point j, minimal thickness and maximal thickness, respectively.

In order to limit the maximum overhangs of the dam or to control the angle of inclination of the arch thrust, the following restrictions can be imposed on the design variables:

$$\pm s_i - c \leq 0 \quad \text{or} \quad \pm s_i \pm s_j - c \leq 0 \tag{6}$$

Stress constraints have the form,

$$\sigma_i + \sigma_{\min} \leq 0 \quad \text{or} \quad \sigma_i - \sigma_{\max} \leq 0 \tag{7}$$

The stresses σ_i in the constraint function may be of any type, i.e. normal and shear stress in global coordinates, normal and shear stress on a prescribed plane (defined through the local parametric coordinate system) and principal stress.

Global load and overturning moment constraints need to be introduced to ensure the overall stability of the dam.

OPTIMIZATION METHODOLOGY

The convex approximation approach to structural synthesis is now widely employed to solve optimal sizing problems, that is to find the design variables that minimize the volume of a structure. When this mathematical programming problem is formulated in the space of the reciprocals of the design variables, it converges much faster to a solution. These properties are generally due to the tendency of the behaviour constraints to be much less nonlinear in the space of the reciprocal variables, while the objective function is strictly convex.

When dealing with shape optimal design problems, the intuitive choice of reciprocal variables is no longer valid. There is indeed no reason why the constraints should be more shallow with respect to the reciprocals of the nodal coordinates. Furthermore, the volume of the structure is no longer a linear function of the shape (design) variables. For these reasons, various approximation schemes have been tested:[14]

(a) first order expansion of the objective function and constraint functions, with respect to the direct variables;

(b) second order expansion of the objective function and linearization of the constraint functions, with respect to the direct variables;

(c) second order expansion of the objective function with respect to the direct variables and linearization of the constraint functions with respect to the reciprocal variables;

(d) linearization of the objective function with respect to the direct variables and linearization of the constraint functions with respect to the reciprocal variables.

Because it has been found that no major benefit can be gained from using a second order expansion of the objective function, this paper will only consider the first and last types of approximation.

1 *Sequential linear programming*

The sequential linear programming approach[12, 13] proceeds by replacing the primary nonlinear problem with a sequence of linear subproblems. Each problem is generated by linearizing the objective function $v(s)$ and the nonlinear constraints $g_i(s)$ about a design point $s^{(k)}$. Using Taylor expansion and neglecting higher order terms,

$$v(s^{(k+1)}) \cong v(s^{(k)}) + (s^{(k+1)} - s^{(k)})^T \nabla v(s^{(k)}) \tag{8}$$

$$g(s^{(k+1)}) \cong g(s^{(k)}) + (s^{(k+1)} - s^{(k)})^T \nabla g(s^{(k)}) \tag{9}$$

where $\nabla v(s^{(k)})$ and $\nabla g(s^{(k)})$ denote the gradients of the objective function and constraint functions with respect to all shape variables at the design point $s^{(k)}$.

Because the resulting explicit problem is a linear programming problem it can be solved by using the Simplex algorithm. Since the optimal solution point corresponds to each linear subproblem necessarily lies at a vertex of the design space, the overall optimization process may either converge to a non-optimal solution of the primary problem or it may oscillate indefinitely between two or more verticles. In order to avoid this undesirable behaviour, the so-called move-limits strategy[15] can be implemented. It consists of temporarily adding some artificial side constraints to the linearized problem so that the design point will not move too far away from the current linearization point $s^{(k)}$. It is, however, very difficult, even for an experienced user, to define adequate rules for setting the move limits and the way they should be adapted after each iteration.

2 *Constraint linearization in the reciprocal space*

This approach consists of keeping the linear approximation of the weight objective function in terms of the original design variables, while linearizing the behaviour constraints with respect to the reciprocals of the design variables:

$$z_j = l/s_j \;;\; j = 1, \ldots \text{NSV} \tag{10}$$

The approximate behaviour constraints take the following form:

$$g(z^{(k+1)}) \cong g(Z^{(k)}) + (z^{(k+1)} - z^{(k)})^T \nabla g(z^{(k)}) \tag{11}$$

where $z^{(k)}$ denotes the current design point in the space of the reciprocal variables. This technique generates at each iteration an approximate problem of the form:

$$\min \sum v_j s_j \tag{12}$$

$$st \sum g_{ij}/s_j \leq g_i \tag{13}$$

$$s_j^L \le s_j \le s_j^U \tag{14}$$

where the g_{ji} coefficients represent first derivatives of the constraint functions with respect to the reciprocal variables (i.e. components of $\nabla g(z^{(k)})$). When restated in terms of the reciprocal variables z_j, the problem involves only linear constraints, and therefore can be solved using a gradient projection algorithm, converging quickly to the solution.

Since the explicit problem is convex and separable, it lends itself to a solution by an extension of the dual method approach.[16] On the basis of the duality theory for convex programming, the solution of the explicit problem is obtained very quickly by a min-max two-phase procedure.

3 *Global and local optima*

The constraint functions form a hypersurface in the NBC design space. Any solution must lie on the surface and the optimum solution lies at the lowest point on the surface. However, the surface may consist of several peaks of varying height surrounded by valleys so that the optimization may fall on a secondary peak. The only solution at present is to take several starting points and choose the best result found.

SHAPE REPRESENTATION

In the geometrical representation of a three-centered arch dam,[1, 2] the horizontal coordinates x and y of the upstream or downstream faces are given by mathematical expressions in terms of the parameters Φ, a, b, R and m which are functions of the vertical coordinate z (Figs 2, 3 and 4):

Central arches:

$$x^2 + (y-a)^2 = R^2 \quad \text{for } \Phi < \Phi_c \tag{15}$$

Lateral arches:

$$(x + b\sin\theta_c)^2 + (y - q + b\cos\theta_c)^2 = R^2 \quad \text{for } \Phi > \Phi_c \tag{16}$$

Radii:

$$R = R_o - a + m \tag{17}$$

Centers position:

$$a + f_1(z) \;;\; b = f_2(z) \tag{18}$$

Vertical profile:

$$m = f_3(z) \tag{19}$$

where normally polynomials are used for the functions f_1, f_2 and f_3.

It is thus necessary to find the following parameters:

(a) central angle defining the limits to the central zone. This angle has been taken as equal for all the arches and for the upstream and downstream surfaces;

(b) four constants in the cubic parabola which defines the variation of $a_m = a_j$ with the height z (the 0th degree term is R_o);

(c) constant value of b_m for all the arches;

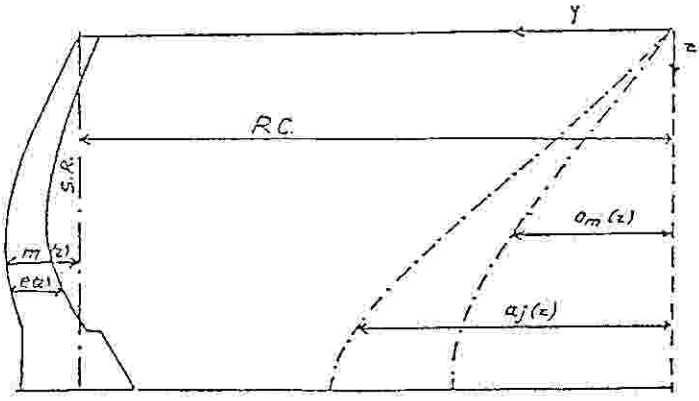

Figure 2.

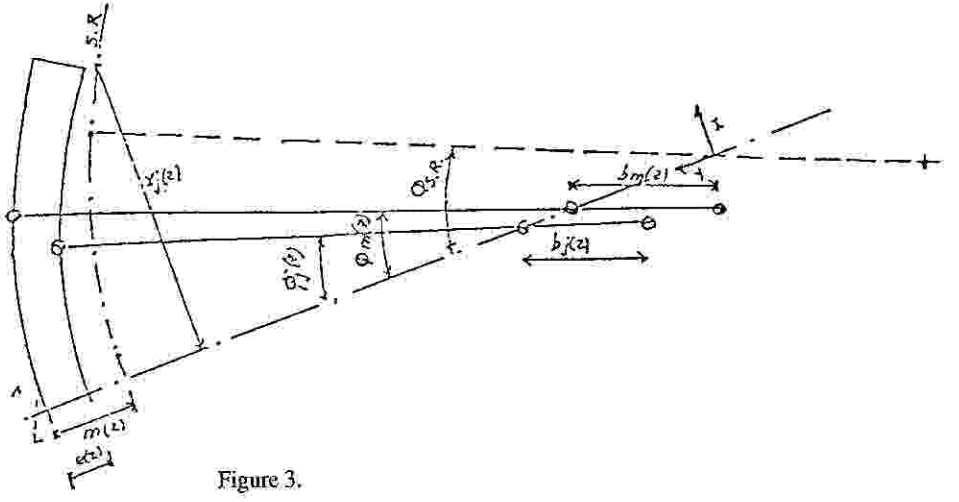

Figure 3.

(d) constant C in the expression defining b_j in the side zones of the dam

$$b_j = b_m - cz$$

(e) four constants of the third degree equation which defines the variation of the thickness with the height;

(f) three constants of the third degree equation which defines the variation of the thickness with the height.

This representation is not easy to implement in the optimization algorithm, since it is not easy to establish analytical relationships between the parameters, therefore causing a numerical instability.

The way to describe the shape of the structure is the key element in the process of obtaining the optimal shape. If the shape variables are not carefully selected, the reliability of the results may be seriously affected.

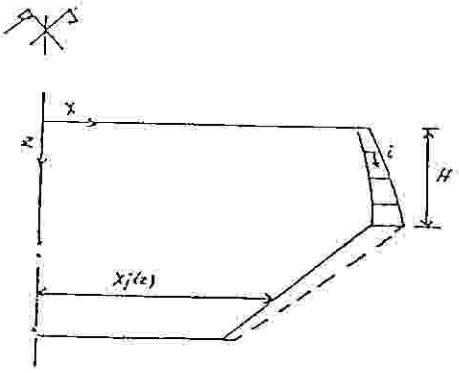

Figure 4.

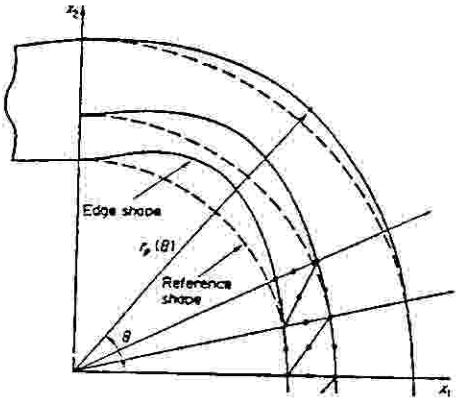

Figure 5.

Three methods for the shape representation are presented in this work:

1. boundary nodes are used for shape representation;
2. the boundary shape is described by piecewise polynomials;
3. the boundary shape is described by spline or spline blending functions.

1 *Boundary nodes for shape representation*

Use of coordinates for boundary nodes in the FE model as shape variables is the earliest and simplest method used. This choice of design variables has, however, severe drawbacks:

(a) The number of design variables becomes very large, which leads to a difficult optimization problem to solve.

(b) It is difficult to ensure compatibility and slope continuity between boundary nodes, which generally leads to inconvenient shapes.

(c) The finite element mesh may need to be changed during the optimization process in order to give accurate results.

2 *Polynomial representation*

In this formulation, a few boundary nodes may be used to control the boundary shape coordinates or moving directions of the control nodes may be used as design variables. Shape functions are used to define the shape of the boundary between control nodes.

In the geometrical form represented in Figure 5, polynomial coefficients are used as shape variables in the system of polar coordinates (r, θ), i.e.:

$$r(\theta) = r_0(\theta) + \sum_{i=1,I} x_i f_i \;\; ; \;\; 0 \le \theta \le \theta_0 \tag{20}$$

Here f_i are smooth functions satisfying relevant end conditions, r_0 is the reference shape function and x_i are the I design variables.

Defining the curves,

$$r_p(\theta) = C_p r_0(\theta) + c_p \sum_{i=1,I} x_i f_i(\theta) \tag{21}$$
$$0 \le \theta \le \theta_0 \;\; ; \;\; p = 1, \ldots P$$

that together with the former equation, define the position of the nodal points by intersection with lines of constant θ. The constants C_p and c_p which satisfy the requirements,

$$1 < C_1 < C_2 < \ldots < C_p \;\; ; \;\; 1 \ge c_1 \ge c_2 \ge \ldots \ge c_p \tag{22}$$

are chosen so that the finite element mesh will not degenerate.

Use of the polynomials with control nodes for shape representation can reduce the total mount of shape variables, but may result in numerical instability if high order polynomials are used.

3 *Spline representation*

Spline as a shape representation can eliminate the problem created by using high order polynomials to describe the boundary, because spline functions are composed of low order polynomial pieces which are combined to maximize smoothness.

A Bezier function is associated with the vertices of a polygon which uniquely define the curve shape. Only the first and last vertices of the polygon actually lie on the function curve; however, the other vertices define the derivatives, order and shape of the function curve. Thus, the curve is defined by an open polygon, as shown in Fig. 6:

$$P(x) = \sum_{i=0,n} P_i J_{n,i}(x) \quad ; \quad 0 \le x \le 1 \tag{23}$$

where,

$$J_{n,i}(x) = [\sum_{i=1,n}] \, x^i (1-x)^{n-i} \tag{24}$$

$$[\sum_{i=1,n}] = n!/[i!(n-i)!] \tag{25}$$

n is a degree of the polynomial and P_i are the $n+1$ defining polygon vertices.

The Bezier function offers many interesting properties such as variation diminishing, axes independence and multiple values, which increase the flexibility of the Bezier function. But it possesses two drawbacks. First, the number of control points fixes the degree of the polynomial which defines the curve. Second, they do not provide local control: moving any control point will change the shape of every part of the curve.

B-splines share many of the characteristics of the Bezier curves. The main advantages of the B-splines are their local control behaviour. They also allow the order of the

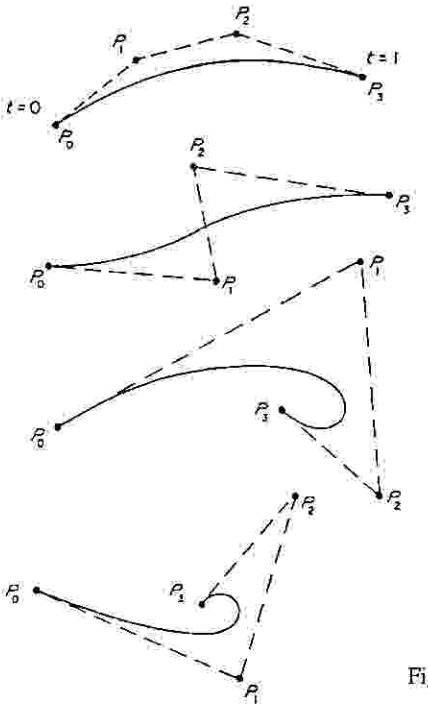

Figure 6.

resulting curve to be changed without changing the number of defining polygon vertices (Fig. 7) and multiplicities of control points.

$$P(x) = \sum_{i=0,n} P_i N_{i,k}(x) \;;\; 0 \le x \le x_{\max} \tag{26}$$

where,

$$N_{i,1}(x) = \begin{cases} 1 \text{ if } X_i \le x \le N_{x+1} \\ 0 \text{ otherwise} \end{cases} \tag{27}$$

$$N_{i,k}(x) = \frac{(x - X_i)N_{i,k-1}(x)}{X_{i+k-1} - X_i} + \frac{(X_{i+k} - x)N_{i+1,k-1}(x)}{X_{i+k} - X_{i+1}} \tag{28}$$

P_i are the $n + 1$ defining polygon vertices, k is the order of the B-splines and $N_{i,k}(x)$ is called the weighting function. X is an additional knot vector which is used for B-spline curves to account for the inherent added flexibility. A knot vector is simply a series of real integers X, such that $X_i \le X_{i+1}$ for all X_i. They can be used to indicate the range of the parameter x used to generate a B-spline curve with $0 \le x \le x_{\max}$ ($x_{\max} = n - k + 2$). The order of a curve is reflected in the knot vector.

4 *Geometric relationship*

A limited number of master nodes (Fig. 8), which control the shape of a subregion or a design element, are selected. These master nodes may lie on the boundary or within the design element or on a certain location outside the design element. The coordinates or

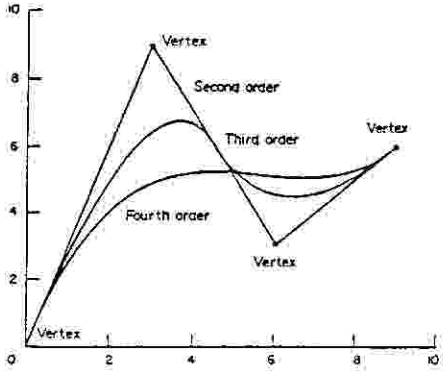

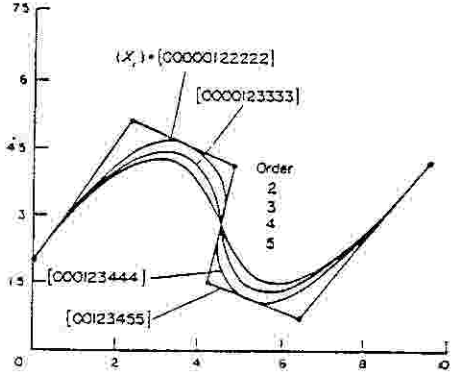

Figure 7.

moving directions of master nodes are the shape variables. The connection of these master nodes with spline blending functions (polynomials, straight lines or other kinds of curves) forms a coarse mesh and a set of design elements. Then each design element is automatically subdivided into several finite elements. For the facility, two local parametric coordinate systems are defined: one of them corresponds to a design element, another to a finite element.

The global coordinates of any point in a design element for the three-dimensional elastic bodies are defined as:

$$\begin{bmatrix} X \\ Y \\ Z \end{bmatrix} = \sum_{j=1,NMN} P_j(\xi,\eta,\zeta) \begin{bmatrix} X_j \\ Y_j \\ Z_j \end{bmatrix} \tag{29}$$

where X, Y and Z are the global coordinates for any point: ξ, η, ζ are the local parametric coordinate system corresponding to the design element; $P_j(\xi, \eta, \zeta)$ are the shape functions defined by the master nodes (X_j, Y_j, Z_j) with spline blending functions or other kinds of curved functions. *NMN* is the number of the master nodes.

The global coordinates for any point in a finite element for three-dimensional elastic bodies are defined as:

$$\begin{bmatrix} X \\ Y \\ Z \end{bmatrix} = \sum_{i=1,NEN} N_i(r,s,t) \begin{bmatrix} X_i \\ Y_i \\ Z_i \end{bmatrix} \tag{30}$$

where $N_i(r, s, t)$ are the shape functions defined by the element nodes (X_i, Y_i, Z_i) which are calculated using the former equation; r, s and t are the local parametric coordinate system corresponding to a finite element and *NEN* is the number of the element nodes.

STRUCTURAL RESPONSE AND SENSITIVITY ANALYSIS

In a finite element displacement approach, the structural analysis consists of solving the

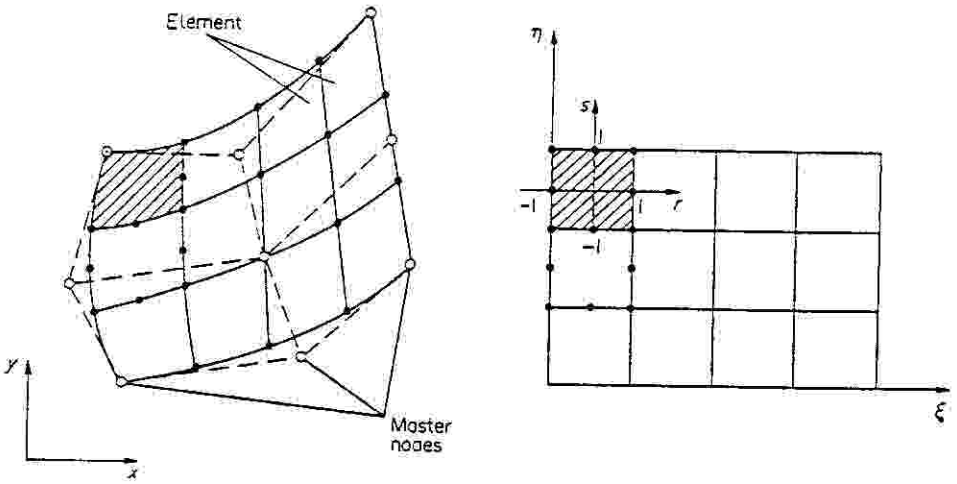

Figure 8.

following equilibrium equations

$$K u = \lambda \tag{31}$$

where K is the structural stiffness matrix, formed by assembling all elements stiffness matrices K_e, u is the unknown nodal displacement matrix, and λ the generalized load vector including self-weight of the structure, hydrostatic pressure or thermal loads. Both K and λ are functions of the shape variables s_k. The major part of the cost of analysis is in the solution of Equation 31 and various numerical techniques may be used to obtain the nodal displacements. Once the nodal displacements are determined, all other structural responses can be sequentially calculated.

A displacement d can be expressed as a linear combination of u, i.e.:

$$d = C^T u \tag{32}$$

where C is a constant matrix for all load cases.

The stress matrix at a certain point belonging to one of the finite elements can also be written as:

$$\sigma = C_e^{\sigma} u_e \tag{33}$$

where C_e^{σ} is the element stress matrix depending on the element nodal forces and on the element stiffness matrix; u_e is the element nodal displacements.

By using the isoparametric finite element technique based on Equation 31, the stiffness matrix K_e, stress matric C_e^{σ} and nodal force vector λ_e are readily written. The global displacements U, V, W for any point in a three-dimensional finite element are expressed as:

$$\begin{bmatrix} U \\ V \\ W \end{bmatrix} = \Sigma_{i=1,NEN} N_i(r,s,t) \begin{bmatrix} U_i \\ V_i \\ W_i \end{bmatrix}$$

i.e.:

$$u = N u_e \tag{34}$$

The strain in any point is:

$$\varepsilon = L N u_e = B_e u_e \tag{35}$$

The element stress matrix is:

$$C_e^{\sigma} = D B \tag{36}$$

where D is the elastic matrix.

The element stiffness matrix is:

$$\begin{aligned} K_e &= \int\int B^T D B \, \mathrm{dv} \\ &= \Sigma_k B_k^T D B_k \det J_k w_k \end{aligned} \tag{37}$$

where k stands for the Gaussian integration points, $\det J_k$ is the Jacobian determinant and w_k the weighting coefficient at k. The nodal force vector is:

$$\begin{aligned} \lambda_e &= \int\int N^T b \, \mathrm{dv} + \int N^T p \, \mathrm{ds} \\ &= \Sigma_k N_k^T b_k \det J_k w_k + \Sigma_l N_l^T p_l \det J_l w_l \end{aligned} \tag{38}$$

where N_k (N_l) denotes the shape function N at point k (l), b_k (p_l) are the volume (surface) forces acting on the point k (l).

1 *Sensitivity analysis*

Design sensitivity analysis, that is the calculation of quantitative information on how the response of a structure is affected by changes in the variables that define its shape, is a fundamental requirement for shape optimization. The first partial derivatives of structural response quantities with respect to shape variables provide the essential information required to couple mathematical optimization methods with structural analysis procedures.

There are two basic approaches to the calculation of sensitivity derivatives. The first is based on differentiation of the discretized finite element system and the second on variation of the continuum equations. This paper presents only the first.

By differentiating Equation 31 with respect to s_k:

$$\frac{\partial u}{\partial s_k} = K^{-1}\left(\frac{\partial g}{\partial s_k} - \frac{\partial K}{\partial s_k} u\right) = K^{-1} \lambda p \tag{39}$$

where,

$$\lambda p = \frac{\partial \lambda}{\partial s_k} + \frac{\partial K}{\partial s_k} u = \Sigma_e \left(\frac{\partial \lambda_e}{\partial s_k} - \frac{\partial K_e}{\partial s_k} u_e\right) \tag{40}$$

represents a pseudo-load matrix.

Then, differentiating Equations 39 and 40 with respect to s_k:

$$\frac{\partial d}{\partial s_k} = C^T K^{-1} \lambda p \tag{41}$$

$$\frac{\partial \sigma}{\partial s_k} = \frac{\partial C_e^{\sigma T}}{\partial s_k} u_e + C_e^{\sigma T} (K^{-1} \lambda p)_e \tag{42}$$

Equations 41 and 42 can also be written in another form:

$$\frac{\partial d}{\partial s_k} = Fp^T V \tag{43}$$

$$\frac{\partial \sigma}{\partial s_k} = \frac{\partial C_e^{\sigma T}}{\partial s_k} u_e + (F_p^T V^{\sigma})_e \tag{44}$$

where:

$$V = K^{-1} C \;;\; V^s = K^{-1} C^{\sigma} \tag{45}$$

represent the virtual displacement matrices under virtual loads $K^{-1}C$ and $K^{-1}C^{\sigma}$, respectively.

The pseudo-load technique uses the set of Equations 39, 41 and 42. The evaluation of the derivatives requires the introduction of *NSV* (number of shape variables) × *NLC* (number of load cases) additional pseudo-load vectors. Equations 43, 44 and 45 represent the virtual-load technique, in which the evaluation of the derivatives needs *NBC* (number of behavioural constraints) additional virtual-load matrices. The derivatives of the structural responses obtained by pseudo-load technique is more economical than by using the virtual-load technique, because the number of *NBC* is much greater than *NVS* × *NLC*.

AUTOMATIC MESH GENERATOR AND REFINEMENT

The second main problem in the shape optimization is the finite element mesh generator and refinement. A fixed element model, as in the sizing optimization, is no longer valid to assure the accuracy of the structural analysis as the shape of the boundary changes, since the accuracy of various portions of the finite element mesh will change. First, it is

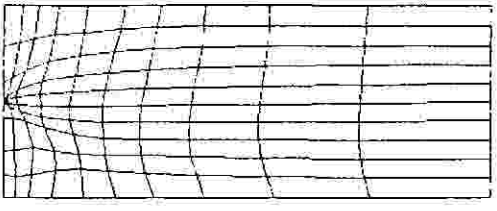

Figure 9.

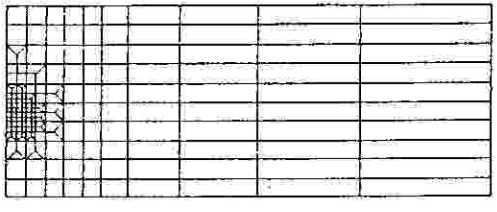

Figure 10.

assumed that techniques exist for automatically generating a finite element mesh for the initial model. Then, information from one structural analysis is used to identify regions of the finite element mesh which need further refinement. The finite element mesh points are relocated whenever the boundary shape changes, and thus individual element distortion due to shape change during the organization process can be kept to a minimum. A natural way of improving the quality of finite element solutions is to increase the number of degrees of freedom. The process is normally performed after an initial solution is already available. Several schemes have been devised to introduce the new degrees of freedom in a selective manner in order to produce the greatest possible improvement over the previous solution.[17] This calls for the definition of a criterion to identify the regions of the domain where the finite element approximation is poorer. The new degrees of freedom are added in these regions either by increasing the order of the polynomial approximation inside elements, the so-called *r*-method, or by subdivision of elements (*h*-method). The process is continued until a specific accuracy is achieved. As a last resort, regenerate the mesh in the whole structure.

1 *r-method*

The *r*-method relocates nodes to satisfy the necessary conditions of optimality without increasing the number of nodes and elements. Furthermore, element connectivities are unchanged during adaptation and the continuity of interpolated functions is assumed without special consideration, while the *h*-method must introduce some methods to maintain continuity. Element distortion in itself does not provide the cause of approximation error. If a large distortion is accompanied by a high gradient of stresses, it is natural to generate a large amount of approximation errors. But if distortion occurs in nearly constant stress fields, it would not generate a significant error. The relocation scheme is not the only reducing deviation of error measures in the finite element model, but also smooths given grids if error measures are almost constant.

2 *h-method*

There are two approaches to the implementation of the *h*-method. The first is without regridding the finite element model. That refinement will be based on the initial grid. For this approach, the important thing is to maintain continuity of the interpolated functions. This leads either to the introduction of linear constraint equations or to special refinements for the transition from refined elements to coarse elements.

A more widely used approach is to introduce a special discretization to transite a refined element to the remainder. New element connectivities must be reassigned in both cases. Application of the *h*-method is realistic but must be done with care, because the total number of degrees of freedom increases too quickly.

The refinement reduces the size of the element to $h/2, h/4, \ldots h/2$ m from the original size h where m is the m^{th} adaptation.

Approximate applications of the *r*-method in general provide smooth results although requiring much more computer time. The *r*-method provides almost the same stress distribution as given by the *h*-method, which involves much more elements. Although the *r*-method may not reduce the total approximation error, it reduces the maximum value of error measures significantly.

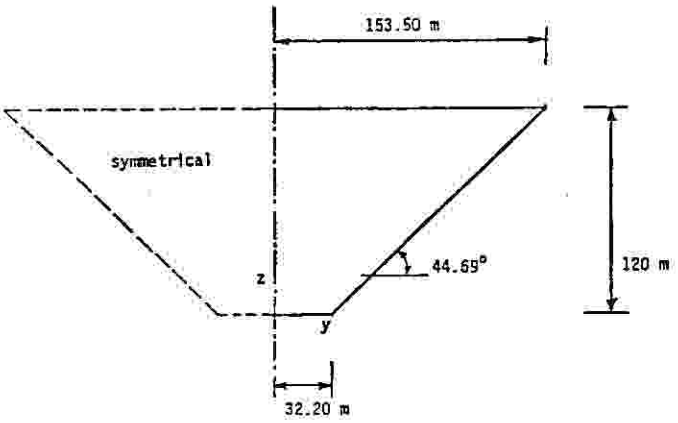

Figure 11.

NUMERICAL APPLICATIONS

The following problem was chosen[7, 8, 12, 13] to illustrate the shape optimization of an arch dam. The dam is designed for combined water (depth 120 m) and gravity loading. The foundation is assumed to have the same elastic properties as the dam ($E = 19{,}600$ MN/m^2, Poisson ratio 0.15).

The type 5 dam[7] was used as a starting shape.* The normal cross-section of the idealized valley is shown in Figure 11.

It is clear that the results reported differ quite substantially as can be seen in the table.

	Volume 10^4m^3	σ_t kN/m^2	σ_c kN/m^2
Type 5 dam	43	4080	–5600
Reference 7	50	2410	–5580
Reference 8	52	2000	–7000
Reference 12	20 or 31†	550	–7000
Reference 13	43	1428	–7428

†There is an apparent different load-carrying behaviour in both designs. If the foundation properties are assumed to be rigid, the arch action dominates in carrying the water load, whereas the cantilever action dominates if the dam-foundation interation is considered (i.e. equivalent static earthquake load and forces produced by fluid flow through the foundation medium are considered in the static analysis).

CONCLUSIONS

The purpose of this paper was to survey shape optimization work with special emphasis

*The shape adopted by the CIRIA Committee on Arch Dams was taken from that of the Cabril dam, Portugal (editors).

on doubly curved arch dams. It was our aim to stimulate ideas leading to future advances in this field. From the numerical examples reported, it is clear that this subject deserves further work.

ACKNOWLEDGEMENTS

The authors thank Professor J. Laginha Serafim for his continued support. Without his efforts and criticism, this work would not have been produced.

REFERENCES

1. Serafim, J.L. 1968. L'évolution de la construction des barrages en beton. *Sciences et Techniques*, no. 11, Paris.
2. Serafim, J.L. 1966. New shapes for arch dams. *Civ. Engng.* 36. New York.
3. Boggs, A.L. 1966. Guide for preliminary design of arch dams. *USBR Engng. Monogr.* 36.
4. Fialho, J.F.L. 1955. Leading principles for the design of arch dams – a new method of tracing and dimensioning. *LNEC*, Lisbon, 65.
5. Brotchie, J.F. 1969. Direct design of arch dams. *Contr. Rev.* 37.
6. Rajan, M.K.S. 1968. Shell theory approach for optimization of arch dam shapes. PhD Thesis, Univ. of California, Berleley.
7. Sharpe, R. 1969. The optimum design of arch dams. *Inst. of Civil Eng.* Paper 7022S.
8. Mohr, G.A. 1979. Design of shell shape using finite elements. *Comp. Struct.* 10, no. 5.
9. Mohr, G.A. 1980. Numerically integrated triangular elements for doubly curved thin shells. *Comp. Struct.* 11, no. 6.
10. Stench, W. & G. Gerry 1975. Free form arch dam design. *J. Struct. Div., Proc. ASCE.*
11. Serafim, J.L., Almeida, L. Tadeu & L. Tavares Valadares 1981. Non-linear parametric optimization of large arch dams. *CESUR.*
12. Wasserman, K. 1983-84. Three dimensional shape optimization of arch dams with prescribed shape functions. *J. Struct. Mech.* 11, 465.
13. Ricketts, R.E. & O.C. Zienkiewicz 1984. Shape optimization of continuum structures. In: E. Atreck, R.H. Gallagher, K.M. Ragsdell & O.C. Zienkiewicz (eds), *New Directions in Optimum Structural Design.* J. Wiley, New York.
14. Braibant, V. & C. Fleury 1985. An approximation concepts approach to shape optimal design. *Comp. Meth. Appl. Mech. Engng.* 53, 119.
15. Bhavikatti, S.S. & C.V. Ramakrishnan 1980. Computational efficiency of improved move limit method of sequential linear programming for structural optimization. *Comp. Struct.* 11, 191.
16. Fleury, C. 1979. Structural weight optimization by dual methods of convex programming. *Int. J. Num. Meth. Engng.* 14, 12.
17. Dias, A.R., N. Kikuchi & J.E. Taylor 1983. A method of grid optimization for finite element methods. *Comp. Meth. Appl. Mech. Engng.* vol. 41, 29.

3.3 OPTIMUM DESIGN OF ARCH DAMS

Zhu Bofang, Li Yisheng & Xie Zhao

Experience shows that shape has a great influence on the economy and safety of an arch dam. At present, the shape of an arch dam is determined mainly by the method of 'cut and